JOURNAL OF SOLID STATE CHEMISTRY 52, 45–52 (1984)

Location of Cs Ions in a Hollandite-Related Superstructure

L. A. BURSILL AND JADWIGA KWIATKOWSKA*

School of Physics, University of Melbourne, Parkville, 3052, Victoria, Australia

Received July 1, 1983; in revised form November 14, 1983

The techniques of electron diffraction, high-resolution electron microscopy, and energy dispersive analysis of X-rays are applied simultaneously to preparations of mixed (Cs,Ba)-titanates. It is shown that Cs does not substitute randomly for Ba in the hollandite-related phase $Ba_2Ti_9O_{20}$ but instead forms a Cs-titanate having probable stoichiometry $Cs_2Ti_4O_9$. For some sample preparation conditions ($\leqq$ 1200°C) lamellae of a Cs-titanate phase were observed to coherently intergrow with $Ba_2Ti_9O_{20}$. However, such intergrowths are probably metastable since for preparation temperatures $\geqq$ 1350°C two distinct phases occurred, being essentially pure $Ba_2Ti_9O_{20}$ and $Cs_2Ti_4O_9$. The Cs-titanate phase appears to have structure different than previously reported, since neither single crystal electron diffraction patterns nor X-ray powder patterns could be indexed using unit cell parameters reported previously for $Cs_2Ti_4O_9$.

1. Introduction

The crystal structure of $Ba_2Ti_9O_{20}$ was determined by comparison of experimental high-resolution electron micrographs (HREM) with images calculated using structural models deduced from the micrographs. Lamellae of hollandite-like tunnel structure alternate with $BaTiO_3$-like units, so that Ba ion diffusion along the tunnels is effectively blocked (*1*).

In this paper the degree of solid solubility (if any) of Cs^+ in $Ba_2Ti_9O_{20}$ is investigated. This is important in view of possible immobilization of ^{137}Cs, a hazardous radionucleide (half-life 33 years) by-product of nuclear technology. HREM is used to investigate the Cs-distribution through its effect on the microtexture of the $Ba_2Ti_9O_{20}$ phase and *in situ* energy dispersive X-ray analysis (EDXA) is used to correlate microtexture with Cs distribution. However, it is found that mixed (Ba,Cs)-hollandite-related phases occurred only for a specific specimen preparation condition. In general it appears that the stable phases are $Ba_2Ti_9O_{20}$ and $Cs_2Ti_4O_9$, which do not readily intergrow. Single crystal electron diffraction and X-ray powder diffraction data are given for the latter phase.

* On leave from the Institute of Nuclear Physics, Radzikowskiego 152, 31-342 Krakow, Poland.

2. Experimental

Following the solution of the crystal structure of $Ba_2Ti_9O_{20}$ it was a logical next step to attempt to replace some of the barium cations by cesium. Inspection of the structure (see Ref. (*1*), Fig. 8b) showed that a sequence of sites

(—Ba—□—Ba—O)

occurs along the "hollandite" tunnels, where O indicates oxygen and □ vacant sites. There are two other Ba sites per tun-

0022-4596/84 $3.00

TABLE I

PREPARATION CONDITIONS FOR Cs-TITANATE PHASES

Specimen number	Initial stoichiometry	Temperatures used	Cooling history
1	$Ba_3Cs_2Ti_{18}O_{40}$ (Carbonate)	1000°C, 4 hr (air) + 1150°C, 17 hr	Slowly cooled Quenched to *RT* ~30 sec
2	$Ba_3Cs_2Ti_{18}O_{40}$ (Carbonate)	1000°C, 4 hr (air) + 1150°C, 17 hr + 1350°C, 18 hr	Slowly cooled Quenched Slowly cooled
3	$Cs_2Ti_{18}O_{37}$ (Carbonate)	800°C (Argon) 3 hr + 1000°C, 3 hr (air)	Slowly cooled
4	$Cs_2Ti_{18}O_{37}$ (Nitrate)	1000°C (air) 3 hr	Slowly cooled
5	$Cs_4Ti_9O_{20}$ (Carbonate)	800°C, 4 hr (air) + 1000°C, 1 week	Quenched
6	$Cs_2Ti_4O_9$ (Nitrate)	1000°C, 36 hr	Slowly cooled
7	$Cs_2BaTi_8O_{18}$ (Nitrate)	1000°C, 26 hr	Quenched

nel, substituting for O in the framework. It therefore seemed most likely that one of the Ba^{2+} ions in tunnel sites could be replaced by two Cs^+ cations, giving overall stoichiometry $Ba_3Cs_2Ti_{18}O_{40}$ for maximum replacement, leading to occupancy of all tunnel sites by Ba, Cs, or O.

A sample of this stoichiometry was prepared by mixing weighed $BaCO_3$, $CsCO_3$, and TiO_2 powders, pressing pellets (~1.5 g) and heating in enclosed, but not sealed, platinum containers. Heat treatment was 1000°C for 4 hr, followed by 1150°C for 17 hr. This specimen was cooled to room temperature by removing quickly from the furnace tube and placing the container in contact with a cold metal block. Portion of this same preparation was reground and heated at 1350°C for a further 18 hr, after which it was slowly cooled. A third specimen was heated at 1150°C for 6 hr, reground and heated at 1400°C for 3 days, after which time the specimen had totally evaporated.

Some electron microscopic observations indicated that a distinct cesium titanate phase had formed (see Section 3 below). A number of pure Cs-titanate preparations were therefore attempted. These are described in Table I. The stoichiometries were chosen initially to ascertain the limit of solid-solubility of Cs_2O in TiO_2 and to look for the phase $Cs_2Ti_4O_9$ (*2*). These specimens were examined by X-ray powder diffractometry.

Specimens were prepared for electron microscopy by grinding under chloroform, in an agate mortar with pestle, and depositing a drop of the suspension onto carbon lace. Thin edges of wedge-shaped crystal fragments were examined using a high-tilt (±60°, ±45°) side-entry goniometer in a JEOL-100CX electron microscope, operating at 100 kV. Diffraction data were collected from as many zone axes as was possible for each fragment. Two dimensional lattice images were sometimes obtainable with this machine, despite the relatively poor spherical aberration coefficient, C_s = 3.5 mm. X-Ray fluorescence spectra were recorded, wherever practicable, using a KEVEX detector using probe diameters of 500–1000 Å.

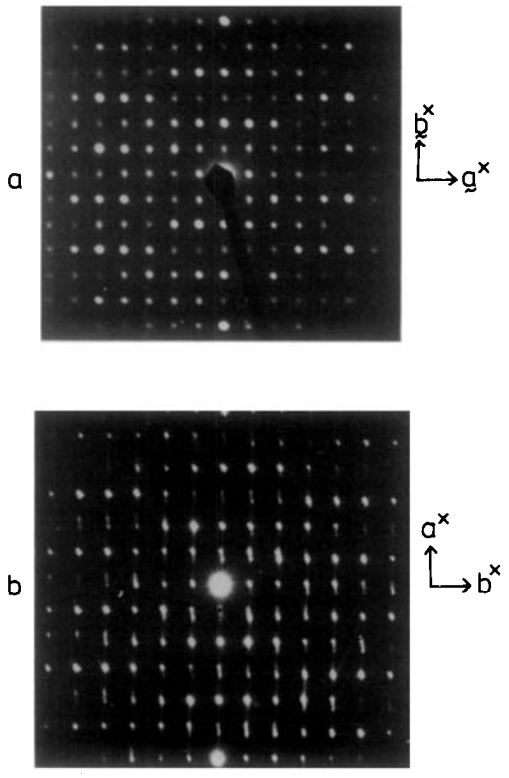

FIG. 1. [001] Zone axis electron diffraction patterns for Ba titanate (a) and mixed (Cs,Ba) titanate (b). Note incommensurate superlattice patterns and orientation "anomalies" in (b).

3. Results

(*a*) *Mixed (Ba,Cs) specimens.* Examination of the first mixed (Cs,Ba) preparation (see specimen 1, Table I) using EDXA showed two distinct spectra corresponding to (i) a pure Ba titanate, having diffraction patterns characteristic of $Ba_2Ti_9O_{20}$ (Fig. 1a); and (ii) a mixed (Cs,Ba) titanate having diffraction patterns characteristic of an intergrowth structure, where incommensurate superlattice spacings and orientation "anomalies" may be seen (Fig. 1b). Figure 1a was readily indexed as the [001] projection of $Ba_2Ti_9O_{20}$ using the triclinic cell parameters $a = 14.36$ Å, $b = 14.10$ Å, $c = 7.48$ Å, $\alpha = 95.5$ Å, $\beta = 100.55°$, and $\gamma = 89.95°$ (*1*). The HREM images corresponding to three mixed (Cs,Ba) crystal fragments are given in Figs. 2a–c. The regular approximately square 14 × 14 Å lattice exhibited by pure $Ba_2Ti_9O_{20}$ (Ref. (*1*), Fig. 2b) becomes heavily faulted in mixed (Cs,Ba) crystals, where lamellae exhibiting a 14 × 7 Å oblique (80°) cell are shown. Many steps occur, where intergrowth lamellae shift plane. The lamellae are mostly quite narrow, lying approximately parallel to [010] and consisting of one or two 14 × 7 Å units. Some wider block-shaped insets of the 14 × 7 Å structure also occur. These are ~5–8 units wide and these may be "crosslinked" by thin bands of dark contrast, indicating a different type of defect structure. Such images proved to be characteristic of mixed (Cs,Ba) titanate fragments. The EDXA spectra corresponding to Figs. 2a–c (inset, Fig. 2) show that increasing Cs/Ba ratio is correlated with increasing density of intergrowth structure. (Analysis of the spectra yielded Cs : Ti ratios of 0.31, 0.49, and 0.66 for Figs. 2a, b, and c, respectively. Errors of ±20% may easily occur in such measurements.)

Examination of the second mixed (Cs,Ba) specimen (number 2 in Table I) showed two distinct phases, one being $Ba_2Ti_9O_{20}$ and the other a cesium titanate. This first became apparent in the EDXA spectra and later in the electron diffraction patterns. The latter were identical with the patterns presented by all of the pure Cs-titanate preparations listed in Table I.

(*b*) *Electron diffraction patterns of Cs-titanate.* Figures 3a, b, and c show three distinct reciprocal lattice sections obtained from specimens 4 and 5. These were generally sharper than those for most other preparations, indicative of the larger crystallite size obtained. However all of the pure Cs titanate preparations showed identical reciprocal lattice geometries. In all cases needle-like fibrous crystallites were obtained. Tilting experiments were made difficult by an apparent continuity in intensity in recip-

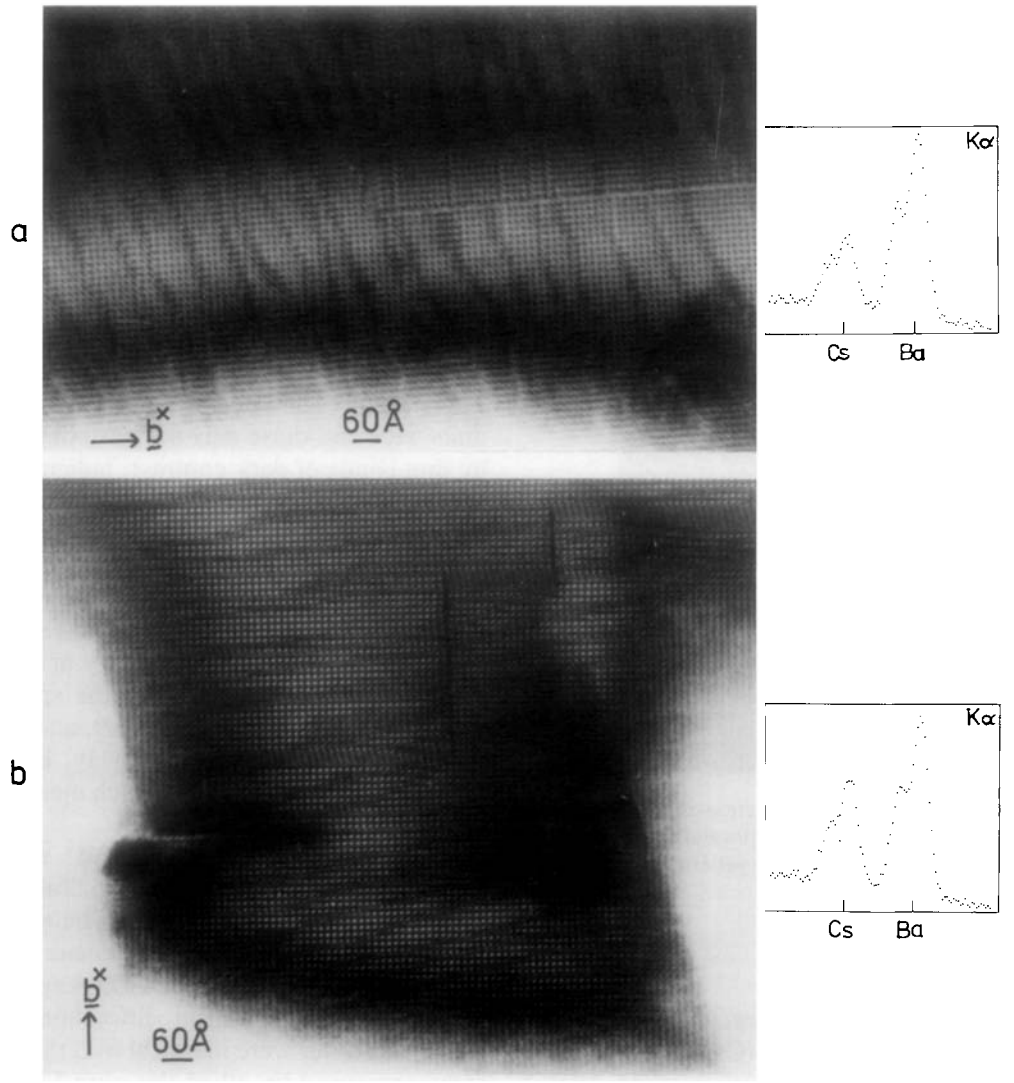

FIG. 2. (a,b,c) HREM images mixed (Cs,Ba) titanate fragments. Note regular 14 × 14 Å square lattice containing intergrowth defects and lamellae of 14 × 7 Å oblique (80°) lattice. The corresponding EDXA spectra indicate increasing Cs–Ba ratio correlates with increasing density of intergrowth structure.

rocal space. On tilting about the short reciprocal axis lattice row through the origin the intensity of the other rows of spots did not always show the expected decrease in intensity and replacement with new reciprocal lattice rows, corresponding to higher order zone axis projections. Instead, the intensity was often noticeably constant with tilt angle over $\sim \pm 30°$. It eventually became clear, after some HREM images were obtained, that the crystallites often formed bundles containing a range of orientations, and in addition even single crystallites were often severely bent or twisted about the long axis. The diffraction patterns selected for Fig. 3 were much sharper than most of

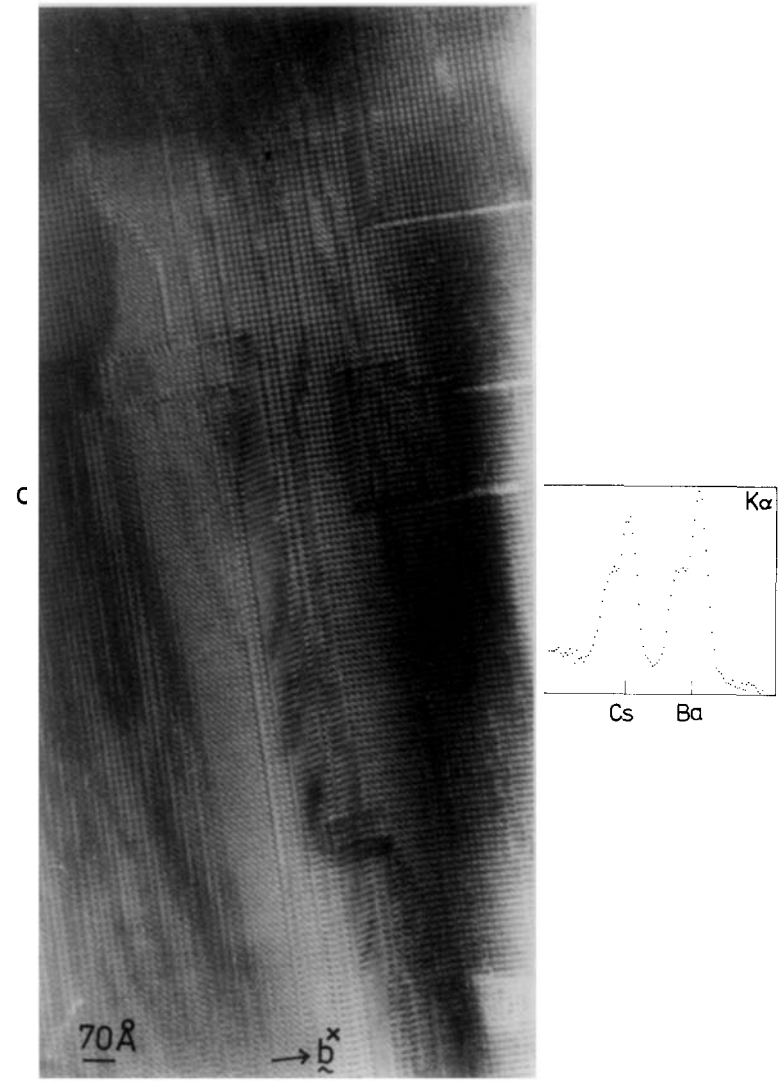

FIG. 2—*Continued.*

those obtained, and should be more suitable for measurements.

(*c*) *X-Ray diffraction patterns of Cs-titanate phase*. Two distinct patterns were obtained throughout the range of starting preparations from TiO_2 to $Cs_2Ti_4O_9$. These corresponded to rutile (TiO_2) and the pattern obtained for $Cs_2Ti_4O_9$ alone. The latter gave *d*-values and relative intensities (Table II) which were quite distinct from those reported in Ref. (*2*).

(*d*) *Electron microprobe analysis of Cs-titanate*. The Cs : Ti ratio was determined to be close to 0.5, by comparison of a polycrystalline aggregate directly with a polycrystalline synthetic preparation having Cs : Ti = 0.5. This result, together with the X-ray powder patterns suggests that the Cs-

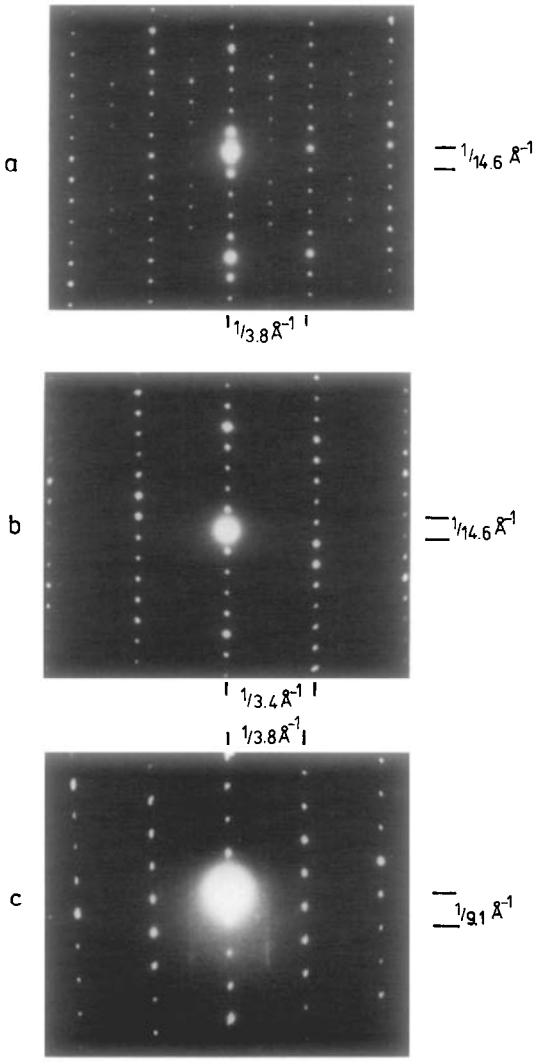

FIG. 3. (a,b,c) Three different zone axis diffraction patterns of pure Cs-titanate phase. Reciprocal lattice dimensions are indicated.

titanate phase has stoichiometry close to $Cs_2Ti_4O_9$.

4. Discussion

(*a*) *Previous work on cesium titanate and related systems.* So far as we are aware the only phase diagram existing for the Cs–Ti–O system was published by Schmitz-DuMont and Reckhard (*2*). Two titanate phases were reported, namely $Cs_2Ti_2O_5$ and $Cs_2Ti_4O_9$. The latter was made by melting $Cs_2Ti_2O_5$ and TiO_2 in a sealed tube. However, no preparations were made in the range $Cs_20.6TiO_2$–TiO_2, it being assumed (on the basis of Debye–Scherrer powder patterns) that $Cs_2Ti_4O_9$ was in equilibrium with TiO_2. Neither unit cell parameters nor crystal structure were reported for $Cs_2Ti_4O_9$, although the Debye-gram was published. A Cs-hollandite phase Cs_xTiO_2 was reported by Lundberg and Andersson (*3*). This phase was prepared by reduction

TABLE II

LIST OF OBSERVED *d*-VALUES AND RELATIVE INTENSITIES FOR $Cs_2Ti_4O_9$ PREPARATION

d (Å)	Relative intensity
10.23	34
(8.85)	(v. weak)
6.47	51
5.93	16
5.68	22
5.09	16
4.96	85
4.67	17
4.25	51
4.06	79
3.97	39
3.81	21
3.35	37
3.32	27
3.19	22
3.03	37
2.95	49
2.93	100
2.87	27
2.85	63
2.68	20
2.61	17
2.54	17
2.37	32
2.27	12
2.23	27
2.12	76
2.05	12
1.90	20
1.70	20

of $Cs_2Ti_2O_5$ in hydrogen at 900°C for a few hours. The tetragonal unit cell parameters were reported as $a = 10.28$ Å, $c = 2.97$ Å. Preparation of $Cs_2Ti_4O_9$ was reported recently (*4*), following ion-exchange of Cs^+ for Tl^+ in $Tl_2Ti_4O_9$ by reaction of CsCl on $Tl_2Ti_4O_9$ at 460°C under 10^{-2} Torr vacuum. The structure was reported as isostructural with $Tl_2Ti_4O_9$ (*5*), with monoclinic unit cell parameters $a = 20.16$ Å, $b = 3.789$ Å, $c = 12.03$ Å, and $\beta = 107.0°$ (space group $C2/m$). The powder pattern was described as being entirely distinct from that reported in (*2*).

Recent work (*6*) has shown that $K_2Ti_4O_9$ may be readily converted into $K_2Ti_8O_{17}$ upon hydrolysis of $K_2Ti_4O_9$, followed by heating at 500°C. A new compound $H_2Ti_8O_{17}$ (believed to have the same octahedral framework structure as $K_2Ti_8O_{17}$) has now been reported (*7*). This was again prepared following hydrolysis of either $K_2Ti_4O_9$ or $Na_2Ti_4O_9$. Intermediate hydrolysis products may be formulated $K_{2-x}H_xTi_4O_9$ ($x \leqq 2$) or $K_{2-x}Ti_4O_{9-x}(OH)_x$. No analogous studies were reported for the Cs-titanates, although one may predict comparable behavior, in view of the well-known hydroscopic and deliquescent properties of cesium oxides. Complete dehydration of $H_2Ti_8O_{17}$ leads to the formation of a phase TiO_2(B), having monoclinic cell parameters $a = 12.163$ Å, $b = 3.735$ Å, $c = 6.513$ Å; $\beta = 107.3$ Å, as first reported in (*6*).

(*b*) *Unit cell parameters for the Cs-titanate phase.* Both the HREM images (Figs. 2a,b,c) and the electron diffraction patterns (especially Fig. 3a, which is virtually identical with the [010] projection of $Ba_2Ti_9O_{20}$ (cf. Ref. (*1*), Fig. 1b), suggested a close relationship of the Cs-titanate to $Ba_2Ti_9O_{20}$. In fact we were able to index the patterns shown in Fig. 3 using a triclinic unit cell $a = 14.35$ Å, $b = 14.38$ Å, $c = 7.20$ Å, $\alpha = 95.5°$, $\beta = 100.6°$, and $\gamma = 78.0°$. This was based upon the reciprocal lattice section (Fig. 3a) having [010] in common with $Ba_2Ti_9O_{20}$. However, when this same cell was used to analyze the X-ray powder pattern (Table II) the agreement between predicted and observed 2θ values was not convincing. In addition we could not find, by electron diffraction, [100] and [001] principal zone axis orientations, despite repeated tilting experiments. It was finally concluded that the pure Cs-titanate phase is not necessarily closely related to $Ba_2Ti_9O_{20}$.

Many attempts have been made to index both the electron diffraction and X-ray powder diffraction patterns using published data for the known Cs-titanate and other alkali-titanate phases (see review in Section 4(a) above). So far our results are inconclusive. The electron diffraction patterns clearly indicate a repeat of ≅14.6 Å, which is ≅5x the 2.97-Å distance characteristic of edge-shared strings of [TiO_6] octahedra, as occur in the rutile, hollandite, $Ba_2Ti_9O_{20}$, and alkali-titanate structures. However, we have not yet been able to identify subcell/supercell relationships which would allow derivation of a unit cell consistent with both the electron diffraction and X-ray powder data.

Further attempts are being made to grow single crystals suitable for X-ray analysis, since the 14.6-Å spacing, which is predominant in electron diffraction patterns, does not occur in the X-ray powder pattern. It is possible that in the vacuum (10^{-7} Torr) of the electron microscope, and perhaps under the influence of the electron beam, there is a change of structure and/or stoichiometry, although we have not been able to obtain definitive electron microscopic evidence for such a change. A degree of hydrolysis, giving $Cs_{2-x}Ti_4O_8(OH)_x$, is one probable chemical change being investigated, since attempts at *in situ* EDXA analysis of pure Cs-titanate preparations were often frustrated by apparent disappearance of the Cs peak on prolonged (≅20–30 min) examination. At the same time there was no

apparent change in the reciprocal lattice geometry.

5. Discussion

It has been shown above that a previously unsuspected Cs-titanate phase exists. It appears to have stoichiometry $Cs_2Ti_4O_9$, but has structure different than reported in Refs. (*2, 6*).

The nature of the Cs-rich phase which was observed to intergrow with $Ba_2Ti_9O_{20}$ in Fig. 2, and its stability requires further investigation. So far it has been found only in preparations heated to 1150°C whereas it is unstable with respect to ($Ba_2Ti_9O_{20}$ + $Cs_2Ti_4O_9$) at higher temperatures. A number of structural models, including $Ba_2Ti_9O_{20}$-related $Cs_2Ti_9O_{18}(OH)_2$ (or $Cs_{2-x}Ti_4O_8(OH)_x$; $x = 1.11$), hollandite-type $Cs_x(Ti_x^{3+}, Ti_{8-x}^{4+})O_{16}$ ($1.33 \leqq x \leqq 1.66$), and the alkali-titanate analog $Cs_2Ti_9O_{19}$ were considered as possibly forming intergrowths with $Ba_2Ti_9O_{20}$. A higher resolution electron microscope study, using computer-simulated image-matching techniques is planned.

From the point of view of radioactive ^{137}Cs disposal it is clear that use of titania-rich "hollandite" preparations (*8, 9*), when the $Ba_2Ti_9O_{20}$ phase may readily occur in SYNROC preparations, needs to be very carefully examined. Use of inappropriate heat treatments may lead to exsolution of ^{137}Cs into the $Cs_2Ti_4O_9$ phase reported here. It cannot be assumed *à priori* that Cs^{+1} randomly and stably replaces Ba^{2+}, either in $Ba_2Ti_9O_{20}$ or in other hollandite-related phases which occur in SYNROC preparations. As shown above the combination of HREM, EDAX, and electron diffraction techniques offers a method for control of the degree of exsolution of various phases which may occur in complex phase assemblages, such as SYNROC.

Acknowledgments

This work was supported by the University of Melbourne, the Australian Research Grants Committee, and the Australian Institute for Nuclear Sciences and Engineering. J. K. is grateful for a University of Melbourne Research Award. The authors thank our colleague Mr. Guido Grzinic for several helpful and fruitful discussions. Dr. Kesson kindly provided a preprint of Ref. (*9*). We are especially grateful to Dr. I. E. Grey and Dr. J. Watts (CSIRO Division of Mineral Chemistry, Melbourne) for electron probe analysis of our preparations which led to the correction of some errors which occurred in an earlier version of this paper.

References

1. G. Grzinic, L. A. Bursill, and D. J. Smith, *J. Solid State Chem.* **47,** 151 (1983).
2. O. Schmitz-DuMont, and H. Reckhard, *Monatsch. Chem.* **90,** 134 (1959).
3. M. Lundberg, and S. Andersson, *Acta Chem. Scand.* **18,** 817 (1964).
4. M. Dion, Y. Piffard, and M. Tournaux, *J. Inorg. Nucl. Chem.* **40,** 917 (1978).
5. A. Verbaere, and M. Tournoux, *Bull. Soc. Chim. (Fr.)* **4,** 1237 (1973).
6. R. Marchant, L. Brohan, and M. Tournaux, *Mater. Res. Bull.* **15,** 1129 (1980).
7. H. Izawa, S. Kikkawa, and M. Koizumi, *J. Phys. Chem.* **86,** 5023 (1982).
8. A. E. Ringwood, S. E. Kesson, N. G. Ware, W. Hilberson, and A. Major, *Nature (London)* **278,** 219 (1979).
9. S. E. Kesson, *Nucl. Chem. Waste Management* (1983), in press.